Biochemical Pharmacology 239 (2025) 117079

Contents lists available at ScienceDirect

Biochemical Pharmacology

journal homepage: www.elsevier.com/locate/biochempharm

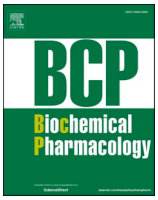

# Givinostat rescues folding of cystathionine beta-synthase and ameliorates murine homocystinuria

Maria Petrosino, Karim Zuhra, Ela Mijatovic, Thilo Magnus Philipp, Olivier Bremer, Kelly Ascenção, Csaba Szabo, Tomas Majtan *

*Section of Pharmacology, Faculty of Science and Medicine, University of Fribourg, Fribourg, Switzerland*

ARTICLE INFO

*Keywords:*
Cystathionine beta-synthase
High-throughput screening
Protein folding
Homocysteine
Pharmacological chaperone

ABSTRACT

Homocystinuria (HCU) is an inherited metabolic disorder caused by missense mutations in the cystathionine beta-synthase (CBS) gene, leading to protein misfolding and degradation. Pharmacological chaperones, which stabilize native protein conformations, offer a promising therapeutic strategy, but tools for their identification are lacking. We developed a cell-based CBS folding reporter assay using split-fluorescent protein complementation, focusing on the common HCU-causing CBS I278T variant. In addition to proteasome inhibitors investigated as potential treatment for HCU, screening of chemical libraries identified several histone deacetylase inhibitors, with givinostat showing the highest recovery of CBS I278T folding and activity. Givinostat binds CBS, but also acts indirectly by modulating the proteostasis network and protein degradation pathways. Short-term treatment of HCU mice expressing CBS I278T partially restored hepatic CBS expression and reduced serum homocysteine levels. This study presents a novel tool, which lead to identification of new class of potential pharmacological chaperones for HCU, paving the way for personalized assays targeting different pathogenic variants and adaptations for other protein misfolding disorders.

## 1. Introduction

Cystathionine beta-synthase (CBS)-deficient homocystinuria (HCU) is an autosomal recessive disorder primarily caused by the presence of missense mutations in the CBS gene, which encodes a crucial enzyme in sulfur amino acid metabolism [1]. CBS is the first enzyme of the transsulfuration pathway where homocysteine (Hcy), a toxic intermediate of methionine metabolism, is irreversibly diverted towards cysteine (Cys) synthesis by its condensation with serine to cystathionine, which is subsequently hydrolyzed by cystathionine-gamma-lyase (CGL) to Cys [2]. Therefore, lack of CBS activity leads to an excessive buildup of Hcy, deficiency of Cys and overall disruption of sulfur amino acid metabolites and persulfidation [3]. HCU affects 1 in 200,000 to 335,000 people worldwide [4]. The clinical impact of CBS deficiency depends on the severity of the disease and may include cognitive impairment, dislocated optic lenses, skeletal abnormalities, and thromboembolic complications. The severity of HCU is correlated with the pathogenic mutation affecting CBS protein and so-called pyridoxine response, i.e. partial rescue of CBS activity by pharmacological doses of pyridoxine, a precursor of the CBS catalytic cofactor pyridoxal-5′-phosphate [5]. In case of pyridoxine non-responsive HCU, the symptoms develop early in childhood and patients have worse prognosis compared to the pyridoxine responsive individuals, which may not show any symptoms until adulthood, where they typically manifest with thromboembolic events [6].

Most of the pathogenic missense mutations causing HCU do not affect key catalytic residues but instead interfere with protein stability, folding and assembly of CBS, often resulting in rapid degradation primarily by the ubiquitin–proteasome system or alternatively aggregation within the cell [7–10]. Protein folding is a complex and dynamic process essential for achieving the fully functional and stable three-dimensional structure. Misfolded unstable proteins are recognized by the cellular proteostasis network, which includes various foldases, isomerases or molecular chaperones to assist and promote the proper folding, assembly and trafficking of the given protein within the cell [11,12]. If the folding attempts fail to yield stable and functional protein, protein degradation pathways of proteostasis network get activated to prevent proteotoxic stress and aggregation, such as ubiquitin–proteasome system or autophagy [13]. Diseases, where the protein homeostasis is impaired by the pathogenic mutations resulting in improper folding,

* Corresponding author at: Department of Pharmacology, University of Fribourg, Faculty of Science and Medicine, Chemin du Musee 18, PER17, Fribourg, 1700, Switzerland.
*E-mail address:* tomas.majtan@unifr.ch (T. Majtan).

https://doi.org/10.1016/j.bcp.2025.117079
Received 13 March 2025; Received in revised form 24 April 2025; Accepted 23 June 2025
Available online 24 June 2025

**Abbreviations**

| | |
|---|---|
| AHA | L-azidohomoalanine |
| AzMC | 7-azido-4-methylcoumarin |
| BRB | bortezomib |
| CBS | cystathionine beta-synthase |
| CD | circular dichroism |
| CETSA | cellular thermal shift assay |
| CFTR | cystic fibrosis transmembrane conductance regulator |
| CGL | cystathionine gamma-lyase |
| Cys | cysteine |
| CTCF | corrected total cell fluorescence |
| DMEM | Dulbecco's modified Eagle medium |
| DMSO | dimethylsulfoxide |
| $EC_{50}$ | half maximal effective concentration |
| ER | endoplasmic reticulum |
| FDA | Food and Drug Administration |
| GFP | green fluorescent protein |
| GIV | givinostat |
| $H_2S$ | hydrogen sulfide |
| HCU | homocystinuria |
| HBSS | Hank's balanced salt solution |
| Hcy | homocysteine |
| HDAC | histone deacetylase |
| HRP | horse radish peroxidase |
| HSP | heat shock protein |
| HTS | high throughput screening |
| IAA | iodoacetamide |
| IRES | internal ribosomal entry site |
| $K_i$ | inhibitor constant |
| KO | knockout |
| LDH | lactate dehydrogenase |
| MG | MG-132 |
| mNG2 | mNeonGreen2 |
| MST | microscale thermophoresis |
| MTT | 3-[4,5-dimethylthiazol-2-yl]-2,5 diphenyl tetrazolium bromide |
| NEM | N-ethylmaleimide |
| PBS | phosphate-buffered saline |
| Phe | phenylalanine |
| PLP | pyridoxal-5′-phosphate |
| PVDF | polyvinylidenedifluoride |
| RFU | relative fluorescence units |
| RIPA | radioimmunoprecipitation assay buffer |
| ROI | region of interest |
| RT | room temperature |
| SEM | standard error of the mean |
| TBS-T | Tris-buffered saline containing 0.1% Tween20 |
| TCEP | Tris(2-carboxyethyl)phosphine |
| tCys | total cysteine |
| tHcy | total homocysteine |
| TSA | thermal shift assay |
| WB | Western blot |
| WT | wildtype. |

reduced stability and/or incorrect assembly, are collectively referred to as misfolding diseases [11,14]. Pharmacological targeting of the cellular proteostasis network has been studied for the development of novel treatments for misfolding diseases as well as other natural processes associated with the dysfunction of protein homeostasis and consequent accumulation of protein aggregates, such as in aging [15], and HCU is no exception. Initial studies with chemical chaperones, such as ethanol, dimethyl sulfoxide or betaine, suggested that folding and activity of many pathogenic CBS mutants can indeed be rescued by the manipulation of a folding environment and cellular proteostasis [16–19]. Later, proteasome inhibitors, such as MG-132 (MG) or the clinically used drug bortezomib (BRB) employed in the therapy of multiple myeloma [20], have shown to rescue of CBS protein and activity and to decrease plasma Hcy levels in murine models of HCU [8,21,22]. However, the long-term use of proteasome inhibitors as therapeutic approach for misfolding diseases is problematic due to the fact that the effective dose of the compound is high, and the associated side effects are significant [23].

Thus, the search for the so-called pharmacological chaperones, small compounds with higher specificity and selectivity for the target than chemical chaperones [24] capable of correcting folding and rescuing activity of misfolded CBS variants, remains of significant importance [25]. Pharmacological chaperones are often represented by substrates, cofactors, inhibitors or other ligands and therefore directly bind the target to stabilize its structure or to induce proper folding. However, indirect, more pleiotropic effects on modulating the cellular proteostasis network have also been described [24,26]. Traditional approaches to identify pharmacological chaperones typically use *in vitro* protein folding assays, such as the thermal shift assay (TSA), with high throughput screening (HTS) of chemical libraries and confirmation of the results by orthogonal assays, such as differential scanning calorimetry or circular dichroism [27,28]. However, these methods are limited by their reliance on isolated proteins (typically only WT variant is available and not the pathogenic mutant, which is not amenable for purification), failing to account for the influence of intracellular environment, compartmentalization and proteostasis network on protein folding, stability and trafficking. To address these limitations, target-specific cell-based assays are necessary for monitoring proper folding and/or protein function within intracellular milieu. The utility of this latter approach is illustrated by the discovery and development of pharmacological chaperones ivacaftor and lumacaftor, which enable the correct folding and trafficking of the certain mutants of cystic fibrosis transmembrane conductance regulator (CFTR) protein in cystic fibrosis [29,30].

Several split-reporter complementation folding/stability assays with a simple readout compatible with HTS have been developed in recent years, such as split-beta-lactamase assay [31] and intra-dihydrofolate reductase enzyme stability assay [32] utilizing rescue of a cell growth as an assay readout. However, assays based on split-fluorescent or chemiluminescent proteins gained most traction in improving folding and stability of the proteins [33–36]. In these latter assays, a reporter protein is typically divided into two non-functional fragments with a smaller fragment being fused with the protein of interest and co-expressed in the cell. When the protein of interest folds correctly, the split fragments reconstitute the functional reporter, yielding a measurable output proportional to the levels of rescued folding/stability. This approach allows for real-time monitoring of protein folding or stability and represents a versatile tool for additional applications, such as improving solubility or studying protein–protein interactions [37].

In this study, we developed a cell-based split-fluorescent CBS folding reporter assay using a yellow-green mNeonGreen2 (mNG2) fluorescent protein, providing an improved ratio of the complemented signal to the background compared to the traditional green fluorescent protein [35]. The assay was evaluated with both CBS WT serving as a control and the most common pathogenic CBS I278T variant by screening the library of FDA-approved drugs. The identified hits were rank-ordered and characterized for their mechanism of action and in mouse model of HCU for their potential to serve as pharmacological chaperones for CBS and eventually as new therapeutic options for HCU.

## 2. Materials and methods

### 2.1. CBS protein

Truncated human CBS lacking the C-terminal regulatory domain (Δ414-551) and carrying permanent 6xHis-tag at its C-terminus (also known as CBS45) was recombinantly expressed in *E. coli* and purified using a two-step chromatographic process as described previously [38].

### 2.2. Plasmids

The CBS folding reporter cassette was codon-optimized and synthesized by Genscript (Rijswijk, Netherlands). The cassette consists of a coding sequence for non-fluorescent $mNG2_{1-10}$ fragment followed by the internal ribosomal entry site (IRES) and a fusion of $mNG2_{11}$ fragment and CBS coding sequences. The N-terminal $mNG2_{11}$ fragment was separated by the recognition site for HRV3C protease, which served as a linker and for an optional removal of the fragment. In addition, CBS contained coding sequence for a 6xHis tag at the C-terminus for optional purification. The synthesized CBS folding reporter cassette was

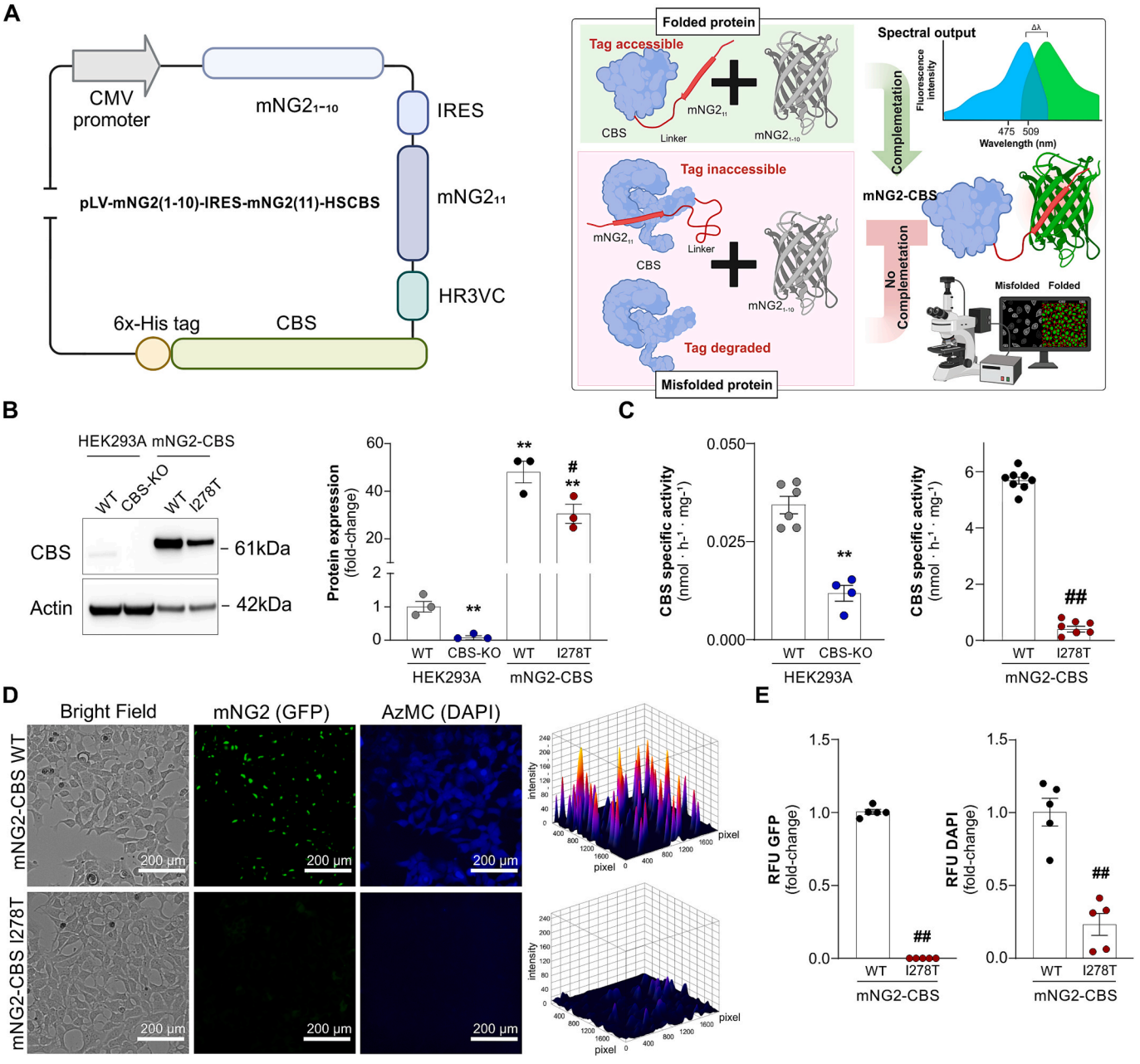


**Fig. 1. Development of a novel CBS folding reporter assay. A –** Schematic of the lentiviral vector used to introduce a CMV promoter-driven bicistronic expression cassette encoding non-fluorescent $mNG2_{1-10}$ fragment and $mNG2_{11}$ fragment N-terminally fused to CBS WT or I278T variant into HEK293A CBSKO cells (mNG2-CBS WT and mNG2-CBS I278T, respectively). Principle of the split-fluorescent protein complementation assay and the applied workflow schematics are shown on the right. **B –** Western blot analysis and quantification of CBS expression in stable cell lines expressing mNG2-CBS WT and mNG2-CBS I278T compared to the CBSKO and WT controls. **C –** CBS activities of the samples shown in panel **B**. **D –** Live-cell imaging of mNG2-CBS WT and mNG2-CBS I278T cells. The mNG2 signal detected in the GFP channel is also presented as 3D surface plots. Live-cell CBS activity determined by the $H_2S$-sensing AzMC probe was detected in the DAPI channel. **E –** Quantification of the mNG2 (GFP) and AzMC (DAPI) signals shown in panel **D**. Data represent mean values ± SEM of at least N = 3 independent replicates. $^{**}P < 0.01$ indicates significant differences compared to HEK293A WT cells. $^{\#}P < 0.05$ and $^{\#\#}P < 0.01$ indicate significant differences compared to mNG2-CBS WT cells.

subcloned into the 3rd generation lentiviral vector (Addgene# 17486; Watertown, MA, USA) directionally into unique SalI and XbaI sites. Schematics of the CBS folding reporter vector is shown in Fig. 1**A**. The pathogenic CBS I278T mutation was introduced by the site-directed mutagenesis by Genscript using CBS wildtype (CBS WT) construct as a template. Both constructs were verified by DNA sequencing performed by Genscript.

### 2.3. Cell lines and cell culture

Supplied plasmids were used for the stable transfection of the previously prepared and characterized HEK293A CBS knockout (CBS-KO) cell line [10]. All HEK293A-based cell lines used in this study were cultured in Dulbecco's Modified Eagle Medium (DMEM; Thermo Fisher Scientific, Basel, Switzerland) containing 4.5 g/l glucose. The medium was supplemented with 10% (v/v) heat-inactivated fetal bovine serum, 2 mM Glutamax, 100 U/ml penicillin and 100 μg/ml streptomycin (all from Thermo Fisher Scientific, Basel, Switzerland). Cells were grown in a humidified incubator at 37°C and 5 %$CO_2$ atmosphere.

### 2.4. Western blot analysis

Western blots (WBs) were performed according to standard protocol. Briefly, clarified cell homogenates (1–20 μg) were separated on a 4–12% Bis-Tris gels (Thermo Fisher Scientific, Basel, Switzerland) and then transferred onto polyvinylidenedifluoride (PVDF) membrane by dry transfer using the iBlot 2 device and the corresponding transfer stacks (Thermo Fisher Scientific, Basel, Switzerland). After blocking with 5% milk in Tris-buffered saline containing 0.1% Tween20 (TBS-T) for 1 h, membranes were incubated with specific antibodies overnight at 4°C. The following antibodies were used (all from CST (Danvers, MA, USA) in 1:1,000 dilution unless indicated otherwise): anti-CBS (#14782), anti-Hsp90 (#4877), anti-Hsp70 (#4872), anti-Hsp60 (#12165), anti-Hsp40 (#4868), anti-Hsp27 (#2402), anti-Hsp22 (#9709) and anti-β-actin (Sigma-Aldrich (St. Louis, MO, USA), A1978, 1:2,000). To test the mouse liver samples, anti-CBS (Proteintech (Manchester, UK), 67861–1-lg, 1:1,000) was used. All the antibodies were diluted in TBS-T containing 5% BSA. After incubation, the membranes were briefly washed 3 times with TBS and incubated for 1 h at room temperature with anti-rabbit or anti-mouse IgG-horse radish peroxidase (HRP) conjugates (CST, #7074 or #7076, respectively) diluted at 1:3,000 in TBS-T with 5% milk. Afterwards, the membranes were washed twice with TBS-T and once with TBS and the detection was performed with ECL Prime reagent (GE Healthcare; Chicago, IL, USA). Chemiluminescence imaging was performed using the Azure Imaging System 300 (Azure Biosystems; Dublin, CA, USA).

### 2.5. CBS activity assay

Hydrogen sulfide ($H_2S$)-producing activity of CBS, utilizing Cys and Hcy, was determined by using a fluorometric assay employing the $H_2S$-selective fluorescent probe 7-azido-4-methylcoumarin (AzMC) as described previously [39]. Briefly, the reaction mixture in a total volume of 200 μl contained 50 mM Tris-HCl pH 8.6, 5 μM PLP, 2 mM Hcy, 10 μM AzMC and 50 μg HEK293A CBS WT or CBS-KO or 5 μg of mNG2-CBS WT or I278T lysates. The plate was incubated for 10 min at 37°C and the assay was triggered by adding 20 mM Cys. The AzMC fluorescence (365/450 nm excitation/emission) was followed for 2 h at 37 °C. All measurements were performed in triplicates using Spectramax M5 microplate reader (Molecular Devices, San Jose, CA, USA) and the data were analyzed using GraphPad Prism software (Boston, MA, USA).

### 2.6. CBS folding reporter assay and HTS

Cells were seeded in black 96-well plates with optical bottom (15,000 cells/well). After overnight incubation, images in brightfield and the GFP channels were acquired using the Cytation 5 imager (Agilent, Santa Clara, CA, USA). At least three biological replicates were performed. The GFP signal quantification was performed either by using Gen5 software (Agilent, Santa Clara, CA, USA) or Image J package (NIH, Bethesda, MD, USA). Analysis with ImageJ was performed starting from the raw 16-bit images in grayscale. We first applied the 'Top Hat' filter with a radius of 50 pixels to enhance local contrast and to subtract background, making differences more prominent. Subsequently, we adjusted the image threshold for each experimental day based on the mNG2-CBS WT cells (positive control) and mNG2-CBS I278T cells (negative control) to ensure precise differentiation between the fluorescent signal and the background. Then, we created a binary mask to isolate the regions of interest (ROIs). To further refine the analysis, we applied the binary operation 'Open' (Process > Binary > Open) to remove any small artifacts and improve the mask's quality. We analyzed the particles using the 'Analyze Particles' function with parameters set to a size range of 2 pixels2 to infinity and a circularity range of 0.00 to 1.00. The lower limit of 2 pixels2 was chosen to exclude very small artifacts and noise, ensuring that only significant particles were included in the analysis. The circularity range of 0.00 to 1.00 allowed us to include all relevant particles, regardless of their shape, ensuring a comprehensive analysis. Finally, we selected all the particles and applied the 'Flatten' function within the ROI Manager to merge all ROIs into a single plane. This step was essential for creating a consolidated image that facilitated further analysis and visualization.

Along with the CBS folding we assessed the CBS activity in live cells using AzMC probe as described previously [10]. Briefly, the replica plate was prepared and treated the same way as described above for the CBS folding reporter assay. However, before fluorescent imaging the culture medium was replaced with Hank's Balanced Salt Solution (HBSS) supplemented with 100 μM AzMC and further incubated for 1 h at 37°C. The AzMC fluorescence was recorder using DAPI channel in Cytation5 imager. Images were analyzed with ImageJ and the corrected total cell fluorescence (CTCF) was determined using the following formula: CTCF = integrated density − (area of the selected cells × mean fluorescence of background readings). Data were analyzed and plotted using GraphPad Prism 8.

The HTS was performed in a similar manner to the above-described CBS folding reporter assay with the following modifications. After overnight incubation of the seeded plate, 2 μl of compounds from the chemical library were added to the medium and gently mixed in. Two libraries were used for HTS: the DiscoveryProbe FDA-approved drug library containing 2,320 FDA-approved drugs (ApexBio (Houston, TX, USA) cat# L1021) and a customized library containing 1,473 compounds (MCE (Monmouth Junction, NJ, USA) cat# HY-LD-000004064). The 0.1% dimethyl sulfoxide (DMSO, vehicle) and 1.56 μM MG-132 (MG) or 10 nM bortezomib (BRB) were used as negative and positive controls, respectively, in each plate. Plates were then incubated for 24 h and processed as described for the CBS folding reporter assay.

### 2.7. CBS half-life determination

Cellular turnover of CBS I278T after treatment with givinostat (GIV; TargetMol, Linz, Austria) was evaluated using a non-radioactive approach based on the incorporation of L-azidohomoalanine (AHA; Sigma-Aldrich, St. Louis, MO, USA), a biorthogonal methionine analog, essentially as previously described [10]. Briefly, HEK293A CBS-KO cells stably expressing CBS WT or CBS I278T mutant were cultured in six-well plates at 50% confluency, and after 6-hours attachment treated with vehicle (PBS) or 10 μM GIV overnight. On the following day, the 4-hour pulse live labeling was performed using 75 μM AHA, which was subsequently replaced by the standard medium containing either vehicle/PBS or 10 μM GIV. The cells were harvested and lysed during the chase period at 0, 2, 6, 9 and 24 h after the pulse. Subsequently, cell lysates (80 μg) were incubated overnight at 4°C with a rabbit polyclonal anti-CBS antibody (1:250) [40] and subsequently pulled down using 25 μl

of washed Pierce protein A/G magnetic beads (Thermo Fisher Scientific, Basel, Switzerland) for 1 h at RT. Immunoprecipitated CBS was conjugated with 10 μM IRDye800-DBCO (LI-COR, Lincoln, NE, USA) for 1 h at RT, and denatured in 2xLDS sample buffer. The AHA/IRDye800-labeled CBS was then resolved in SDS–PAGE and visualized and quantified by fluorescent in-gel detection using the Odyssey DLx imaging system (LI-COR, Lincoln, NE, USA). Fluorescent signal was normalized to total CBS levels and plotted over time. Rate constants and half-lives were then determined using the one-phase decay function in GraphPad Prism software.

### 2.8. Microscale thermophoresis (MST)

The MST assay was performed using a Monolith NT.115 (Nano Temper Technologies, Munich, Germany) as described previously [41]. Briefly, 6xHis-tagged CBS45 was labeled using the RED-Tris-NTA Histag protein labeling kit (Nano Temper Technologies, Munich, Germany), mixed with serial dilutions of givinostat (0–150 μM) in a binding buffer and incubated for 20 min at 30°C. After loading of the samples into glass capillaries and measurement, the dissociation constant $K_D$ was obtained. Experiments were performed in triplicates and the $K_D$ value was obtained using the one site-total binding equation model in GraphPad Prism.

### 2.9. Circular dichroism (CD)

The CD spectra were recorded on a Jasco J-1500CD spectropolarimeter (JASCO Corporation, Tokyo, Japan) equipped with a Peltier-type temperature controller. Near-UV (250–450 nm) CD spectra of 1 mg/ml CBS45 in the absence or presence of 1 μM givinostat were collected at 25°C using 1 cm path-length quartz cuvette at a scan rate of 50 nm/min in a buffer containing 50 mM Tris.HCl pH 8.5, 200 mM NaCl and 200 μM Tris(2-carboxyethyl)phosphine (TCEP; Soltec Ventures, Beverly, MA, USA). A minimum of three accumulations were made for each scan, averaged and corrected for the blank solution of the corresponding buffer. The results were expressed as the mean residue ellipticity ([Θ]), assuming a mean residue molecular mass of 110 per amino acid residue.

### 2.10. Animals and study design

A breeding pair of heterozygous transgenic C57BL6 mice, which are knocked out for mouse CBS and express the human CBS I278T transgene under a zinc-inducible promoter, was generously provided by Dr. Warren Kruger (Fox Chase Cancer Center, Philadelphia, PA, USA) [42]. The breeding pairs were maintained on water supplemented with 25 mM zinc sulfate to induce transgene expression and to rescue the homozygous pups from neonatal mortality. After weaning at 21 days of age, mice were tagged, genotyped, switched to regular water, and provided with an extruded standard diet (3436, Kliba Nafag, Kaiseraugst, Switzerland). Homozygous CBS knockout mice carrying the I278T transgene (Tg-I278T mice) and their siblings with two copies of the mouse CBS gene (WT mice) were used for *in vivo* studies.

For the experiments, 13 animals (3 wt and 10 Tg-I278T mice) between 26 and 34 weeks of age were used. The week prior to the beginning of the experiment (W0), all mice were weighed and handled to promote their habituation to the experimenter. Additionally, the mice were switched from regular water to zinc-supplemented water to until the end of the study to induce the expression of CBS I278T transgene. After the week of acclimation, mice received either vehicle (PBS) or 25 mg/kg/day GIV per orally using micropipette-guided drug administration technique in a total volume of 50–70 μl depending on the weight of the mice using 10% condensed milk as a carrier to facilitate and promote compliance [43]. The treatment was done every day at 10AM for up to 3 weeks, while the dose was adjusted once weekly based on the weights recorded. Blood sampling was performed by submandibular bleeding technique using 5 mm lancet into Serum gel tubes (Sarstedt, Numbrecht Germany) before the treatment period for baseline and then once weekly every Friday at 3PM. At the end of treatment period, mice were terminally bled, euthanized with 150 mg/kg pentobarbital and perfused with PBS. Livers, kidneys and brains were collected and snap frozen in liquid nitrogen. Procedures involving mice were performed according to the animal study protocol 2024–22-FR reviewed and approved by the cantonal veterinary office.

### 2.11. Plasma metabolomics

Total Hcy (tHcy) and total Cys (tCys) were quantified using Probe 1 essentially as described previously [44].

### 2.12. Data analysis and statistics

Data are presented as means ± standard errors of the mean (SEMs) of at least three independent experiments. Statistical analysis was performed using the one-way ANOVA followed by post-hoc Bonferroni's or Tukey's multiple-comparison test. Differences with the $P < 0.05$ (marked as * or $^{\#}$) and $P < 0.01$ (marked as ** or $^{\#\#}$) were considered significant. Curve-fitting, histograms and $EC_{50}$ determinations as well as statistical analysis were performed using GraphPad Prism.

The Z' factor, a statistical criterium whether the screening method satisfies the minimal standards of quality and reliability to be employed as HTS assay, was calculated as described previously [45]. The Z score factor, a statistical criterium to identify significant hits throughout the screening campaign, was determined as described previously [46].

## 3. Results

### 3.1. Development of a novel CBS folding reporter assay

We designed and constructed lentiviral vectors overexpressing non-fluorescent $mNG2_{1-10}$ fragment and $mNG2_{11}$ fragment N-terminally fused to CBS WT (mNG2-CBS WT) or pathogenic CBS I278T variant (mNG2-CBS I278T). These constructs are under the control of a strong constitutive CMV promoter expressed from a bicistronic IRES-mediated cassette. As the expression yield from the 3′ cistron is often lower compared to that from the 5′ cistron, we inserted the CBS-$mNG2_{11}$ cassettes at the 3′ cistron and $mNG2_{1-10}$ at the 5′ cistron to ensure that the CBS-$mNG2_{11}$ is the limiting factor for the mNG2 complementation. Fig. 1**A** shows the schematics of the expression constructs and CBS folding reporter assay. Western blot analysis confirmed that HEK293A CBS-KO cells stable transfected with the designed vectors yielded substantial amounts of CBS for both mNG2-CBS WT and mNG2-CBS I278T (Fig. 1**B**). Notably, CBS levels in mNG2-CBS I278T were significantly lower compared to mNG2-CBS WT likely due to the well-established lower stability and faster degradation of CBS I278T [10]. The CBS activity assay confirmed that there is essentially no baseline CBS activity in HEK293A CBS-KO cells used as a host for the CBS folding reporter constructs (Fig. 1**C**). Expression of mNG2-CBS WT resulted in ~200-fold increase in CBS activity compared to HEK293A WT cells, while mNG2-CBS I278T cells showed substantial impairment in CBS activity (Fig. 1**C**). Live cell fluorescence microscopy confirmed that in mNG2-CBS WT cells, CBS WT was properly folded leading to a complementation of mNG2, which, in turn, yielded a strong and well localized fluorescent signal (Fig. 1**D**). In contrast, in mNG2-CBS I278T cells, expression of CBS I278T variant produced a cell-wide, low-level diffused signal, consistent with the misfolding of CBS I278T, its rapid degradation, and its inability to complement mNG2 (Fig. 1**D**). Decreased levels and low activity of CBS I278T (Fig. 1**B&C**) as well as its impaired folding (Fig. 1**D**) were further confirmed by determining CBS activity in live cells in replica plates of CBS folding reporter assay (Fig. 1**D**). Quantification of fluorescence intensities and distribution within the cells for both the mNG2 (GFP) and AzMC (DAPI) signals confirmed that CBS

I278T misfolds and has very low residual activity within the cellular milieu (Fig. 1**D&E**). The developed CBS folding reporter assay has a Z' factor of 0.88 indicating a robust assay performance and reliability. This value surpasses the generally accepted threshold for HTS applications confirming its suitability and effectiveness for further development and application in HTS.

### 3.2. Validation of the CBS folding-reporter assay

Previous studies demonstrated that proteasome inhibitors, such as MG and BRB (Fig. 2**A**), can rescue stability and activity of CBS I278T in both the cell-based and *in vivo* models of HCU [8–10]. Therefore, we used these compounds to validate our CBS folding reporter assay. After treating the cells with increasing concentrations of these inhibitors for 24 h, we determined that 1.56 μM MG and 10 nM BRB were the most effective concentrations to rescue CBS I278T folding, while avoiding

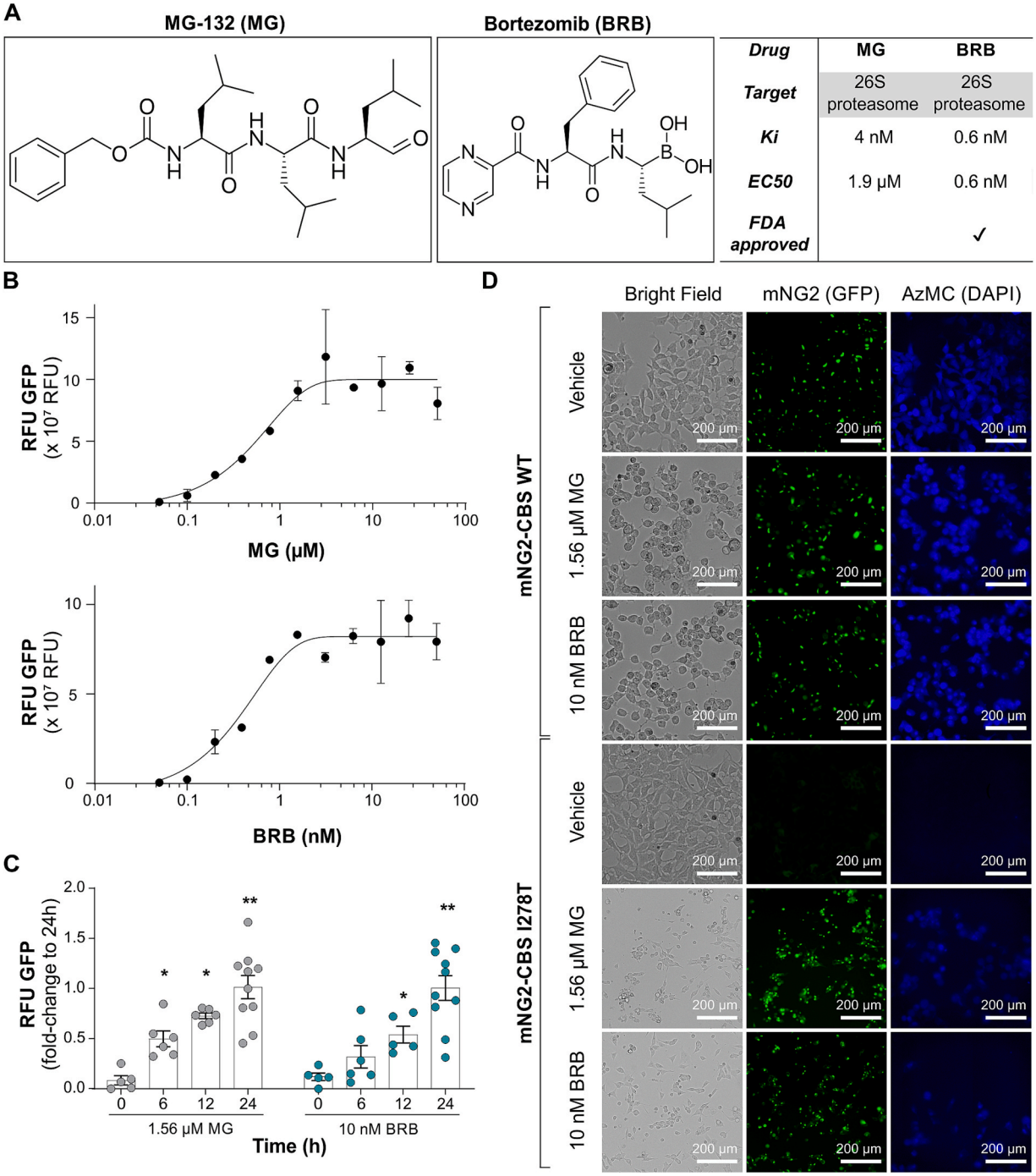


**Fig. 2. Validation of the CBS folding reporter assay. A –** Chemical structure and properties of proteasome inhibitors MG-132 (MG) and bortezomib (BRB). **B –** Dose-response curves of MG and BRB. **C –** Time-dependent response (0–24 h) of MG (1.56 μM) and BRB (10 nM). **D –** Live-cell imaging of mNG2-CBS WT or I278T cells in the absence (Vehicle) and presence of the treatment with MG (1.56 μM) and BRB (10 nM). Representative brightfield, GFP (mNG2-CBS folding) and DAPI (AzMC CBS activity) channels are shown. Data represent mean values ± SEM of at least N = 3 independent replicates. $^{*}P < 0.05$ and $^{**}P < 0.01$ indicate significant differences compared to time 0 h.

cellular toxicity (Fig. 2**B**). Significant improvement in CBS I278T folding was observed already after 12 h of incubation with these compounds but the maximal signal was achieved at the end of incubation i.e. at 24 h (Fig. 2**C**). Treatment of the cells with 1.56 μM MG or 10 nM BRB for 24 h produced a near-complete rescue of the folding of CBS I278T, but CBS activity was only partially restored (Fig. 2**D**). These results confirm the ability of proteasome inhibitors to rescue protein folding and activity of CBS I278T variant, thus validating our assay.

### 3.3. Screening of chemical libraries

Using the CBS folding reporter assay validated above to screen two chemical libraries containing 2,320 FDA approved drugs and 1,473 experimental compounds in various stages in development, to identify novel pharmacological chaperones capable of restoring folding and activity of CBS I278T (Fig. 3**A**). The screening was performed in a 96-well plate format at a single 10 μM concentration and a 24 h treatment period. Each plate contained negative (vehicle-treated mNG2-CBS I278T cells) and positive controls (mNG2-CBS I278T cells treated with 1.56 μM MG or 10 nM BRB), which served as internal controls as well as to set the baseline and to control variations between multiple plates assayed at different days. Based on image analysis validated by the Z score statistical analysis, we identified 33 hits that partially rescued folding of CBS I278T variant (Fig. 3**A&B**). These hits were further evaluated for their ability to rescue catalytic activity of CBS I278T by the cell-based AzMC-based activity assay (Fig. 3**C**). Considering CBS folding and activity recovery together with the biological properties and development stage of the identified hits, we chose givinostat (GIV) for further characterization and its potential to serve as a pharmacological chaperone for HCU (Fig. 3**D&E**). This molecule is a recently approved histone deacetylase (HDAC) inhibitor which represents the first nonsteroidal treatment for Duchenne muscular dystrophy [47].

### 3.4. Functional characterization of givinostat

Detailed analysis and comparison of live cell CBS folding and activity data revealed that 10 μM GIV is as effective in rescuing folding and activity of CBS I278T as the two proteasome inhibitors used as positive controls (Fig. 4**A-C**). Concentration of GIV up to ~10 μM did not substantially impair cell viability as measured by the MTT assay and the LDH release assay (Fig. 4**D**), in contrast to the proteasome inhibitors, which induced detectable cytotoxicity in the same assay (Fig. 4**E**). As anticipated based on the results from CBS folding reporter assay, cellular turnover of CBS I278T variant substantially improved after treatment with 10 μM GIV; the resulting enzyme stability was comparable to the stability of CBS WT (Fig. 4**F**). Specifically, treatment of the cells expressing CBS I278T with 10 μM GIV doubled the half-life of CBS I278T (Table 1). Our subsequent experiments demonstrated that GIV directly binds to the catalytic core of human CBS (CBS45) with $K_D$ value of 30 μM (Fig. 4**G**). Near-UV–VIS (250–700 nm) CD spectroscopy of CBS45 incubated with 1 μM GIV demonstrated that binding of GIV to the protein induces conformational changes that involve mostly the PLP-containing catalytic center, heme moiety and the phenylalanine (Phe) and tyrosine (Tyr) residues. Indeed, addition of 1 μM GIV resulted in a decrease in the molar ellipticity at 410 nm, the positive peak observed for the presence of a PLP cofactor, in an increase of the 280 nm band, the region were Phe and Tyr residues define their contribution and a decrease in the molar ellipticity between 450 and 700 nm, probably due to changes in the heme region (Fig. 4**H**). In addition to the direct interactions of GIV with CBS protein, treatment with 10 μM GIV was accompanied by a differential expression of certain heat shock proteins (HSPs; Fig. 4**I**). Specifically, protein levels of Hsp90, Hsp70, and Hsp40 were increased, while the levels of Hsp27 and Hsp22 were significantly reduced and the levels of Hsp60 remained unchanged (Fig. 4**I**). Taken together, these results indicate that givinostat affects folding, stability and activity of CBS I278T both directly and indirectly.

### 3.5. Confirmation of the efficacy of givinostat in a mouse model of HCU

To translate our *in vitro* cell-based findings into *in vivo* evidence demonstrating that givinostat acts as a pharmacological chaperone being able to rescue folding and activity of CBS mutant and ultimately to restore metabolic balance, we used transgenic CBS I278T-expressing HCU (Tg-I278T) mice. Mice were treated orally with either vehicle or 25 mg/kg/day GIV for a period of three weeks. Expression of CBS I278T in liver after three weeks of treatment was significantly higher compared to vehicle-treated Tg-I278T mice; however, it still remained substantially lower compared to the CBS levels in healthy control mice (Fig. 5**A&B**). Interestingly, assessment of CBS activity in liver homogenates did not correlate well with the partially rescued CBS I278T protein levels, showing only relatively slight increases in CBS activity (Fig. 5**C**). Nevertheless, quantification of tHcy in serum samples showed gradual decrease of plasma tHcy levels in givinostat-treated Tg-I278T mice over the course of treatment, which after three weeks reached a significant 25 % decreased compared to baseline levels of untreated mice (313 μM versus 420 μM, respectively; Fig. 5**D**), while serum tCys levels remained unchanged (Fig. 5**E**). These results indicate that givinostat partially rescues CBS I278T folding *in vivo*, which translates in an improved metabolic balance.

## 4. Discussion

HCU is a rare metabolic disorder [4,48] which has never been in the research spotlight since its discovery in the 1960's. Severe methionine restriction and provision of methionine-free amino acid formula remain a cornerstone approach for pyridoxine non-responsive HCU, which can be somewhat alleviated by betaine supplementation, while milder pyridoxine responsive forms of HCU are effectively managed by pyridoxine supplementation [6]. However, the last decade has seen an increased interest in the development of novel treatments for HCU, which primarily focus on decreasing plasma tHcy levels either by reduction of absorption of its precursor methionine from gastrointestinal tract (SYNB1353, CDX-6512) or degradation of circulating methionine (erymethionase) or homocysteine (pegtibatinase, pegtarviliase) [49]. As of now, only pegtibatinase remains in clinical development. To address the persistent unmet need for better therapeutic options considering that HCU due to the presence of missense pathogenic mutations is a conformational disorder, development of pharmacological chaperones capable of correcting protein folding and restoring the activity of pathogenic CBS variants holds significant scientific and clinical promise [25,49]. Various versions of thermal shift assays (TSAs), which are typically used as the first line screening method in drug discovery, have major limitations for protein misfolding disorders such as HCU [50]. Traditional TSA requires substantial amounts of the purified target of interest, which is possible to satisfy using the WT variant as pathogenic mutants are often unstable, degraded or form insoluble aggregates, which are consequently not amenable for purification. TSA detects only direct interactions of the test compound with the protein of interest, which results in structural stabilization characterized by an increased melting temperature [28]. Therefore, any indirect effects which occur in a cellular milieu, such as modulation of cellular proteostasis network, posttranslational modification or rescued trafficking, cannot be detected by TSAs. To overcome these limitations, thermal shifts were recently also determined in cellular content using cellular TSAs (CETSA), which extend the utility of TSA approach to the full detectable proteome and have a potential to inform about the indirect effects too [50].

Here we developed a split-fluorescent protein CBS folding reporter assay designed to assess both direct and indirect impacts on CBS folding and stability in cellular milieu (Fig. 1). Instead of the originally used green fluorescent protein [33], we used a yellow-green mNG2 fluorescent protein that showed previously strong complementation and improved signal-to-noise ratio [35]. The last beta-strand ($mNG2_{11}$ fragment) is only 16 amino acid residues-long (~1.7 kDa) thus

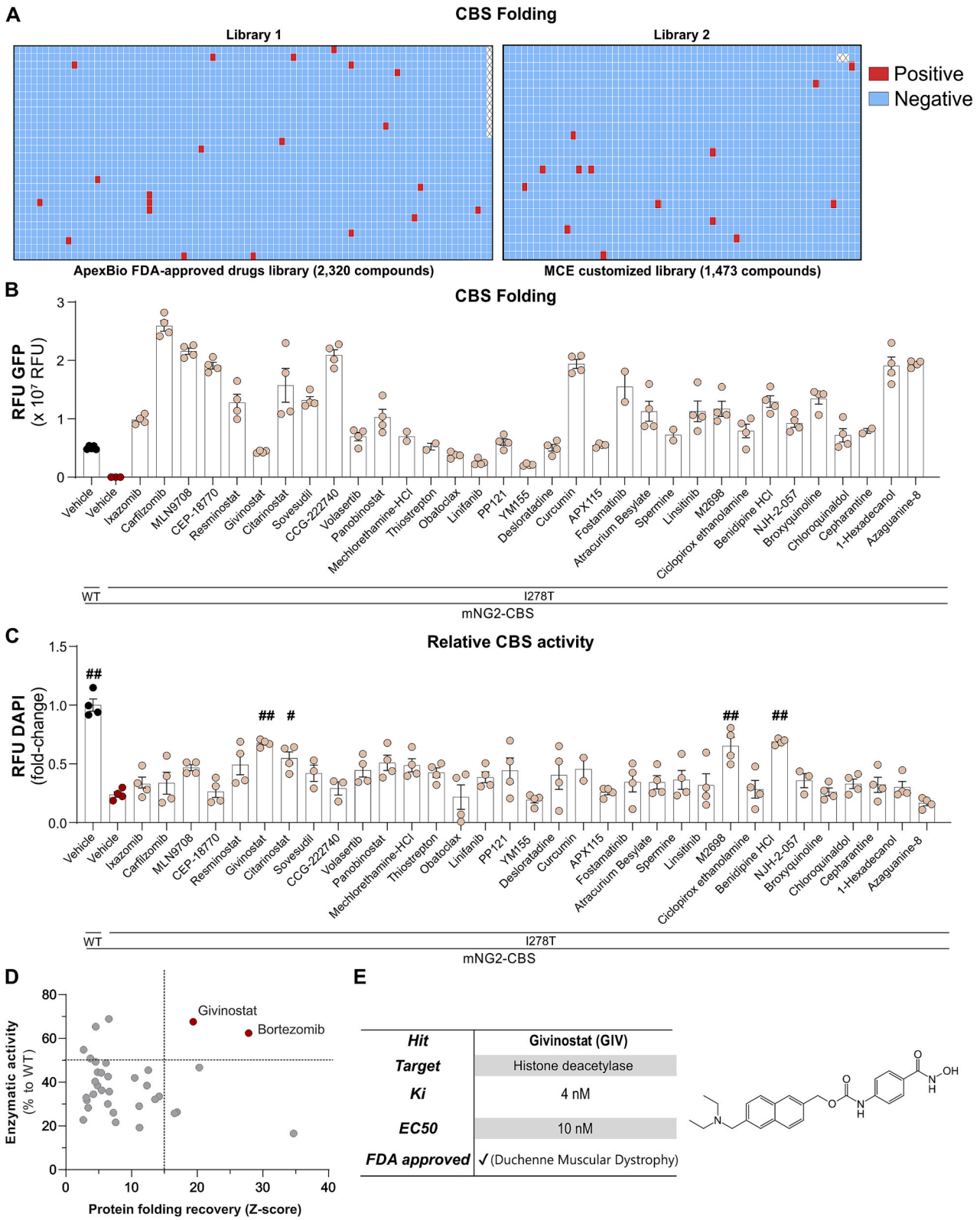


**Fig. 3. Screening of the chemical libraries. A –** Heat maps of ApexBio and MCE chemical libraries containing 2,320 FDA-approved drugs and 1,473 experimental compounds in various stages of development, respectively, obtained from the screening of the mNG2-CBS I278T cells using CBS folding reporter assay. Compounds were tested at a single concentration of 10 μM and the GFP signal was measured 24 h after the treatment. Positive hits (red) improved folding and/or stability mNG2-CBS I278T, while negative hits (blue) did not. **B –** Quantified mNG2 (GFP) fluorescence signal as a measure of proper CBS folding from the positive hits identified in panel **A**. **C –** Quantified AzMC (DAPI) fluorescence signal as a measure of the rescued CBS activity from the positive hits identified in panel **A**. **D –** Recovery of CBS folding expressed as a Z score correlated to the rescue of CBS activity identified givinostat is the best candidate from the hits. **E –** Chemical structure and properties of givinostat (GIV). Data represent mean values ± SEM of N = 4 independent replicates. $^{\#}P < 0.05$ and $^{\#\#}P < 0.01$ indicate significant differences compared to mNG2-CBS I278T cells.

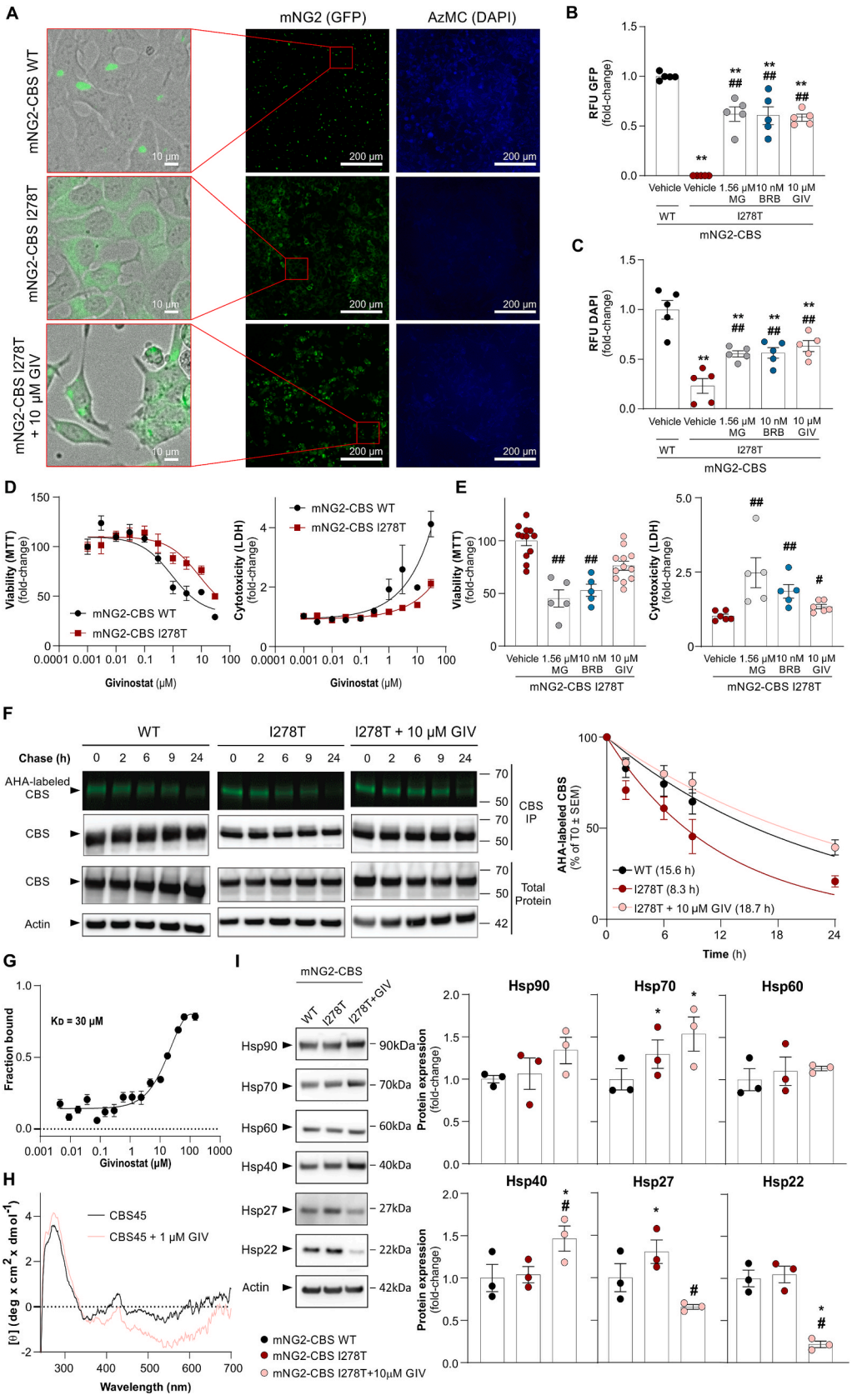


*(caption on next page)*

**Fig. 4. Functional characterization of givinostat. A –** Live-cell imaging of mNG2-CBS WT and I278T cells in the absence or presence of 10 μM givinostat. Representative brightfield, GFP (mNG2-CBS folding) and DAPI (AzMC CBS activity) channels are shown. **B&C –** Quantification of the GFP (**B**) and DAPI (**C**) signals detected in mNG2-CBS WT and I278T cells in the absence (Vehicle) or presence of the treatment (1.56 μM MG, 10 nM BRB or 10 μM GIV). **D&E –** Cell viability (MTT) and cytotoxicity (LDH) assays. **F –** Representative images of fluorescent gels and Western blots for both immunoprecipitated CBS and total protein fractions (500 ng/lane) obtained from cell lysates of HEK293 CBS WT, CBS I278T or CBS I278T treated with 10 μM givinostat at the designated timepoints (0, 2, 6, 9 and 24 h after the AHA labeling). AHA pulse-chase data were normalized for the protein content and CBS expression and fitted to the first-order rate kinetics to yield cellular CBS turnover (Table 1). **G –** Binding of givinostat to CBS45 determined by MST. **H –** Near-UV CD spectra of CBS45 (black) and CBS45 complexed with 1 μM GIV (light pink). All spectra were recorded at 25 °C. **I –** Representative Western blots and quantification analysis of Hsp proteins in mNG2-CBS WT and mNG2-CBS I278T cells in the absence and presence of 10 μM givinostat. Data represent mean values ± SEM of at least N = 3 independent replicates. $^{*}P < 0.05$ and $^{**}P < 0.01$ indicate significant differences compared to mNG2-CBS WT cells. $^{\#}P < 0.05$ and $^{\#\#}P < 0.01$ indicate significant differences compared to mNG2-CBS I278T cells.

**Table 1**
CBS stability rate constants and CBS half-lives.

| Sample | Rate constant ($h^{-1}$ ± SEM) | Half-life (h ± SEM) | $R^2$ |
|---|---|---|---|
| **CBS WT** | 0.044 ± 0.002 | 15.6 ± 0.5 | 0.894 |
| **CBS I278T** | 0.084 ± 0.004 | 8.3 ± 0.4 | 0.903 |
| **CBS I278T + 10 μM GIV** | 0.037 ± 0.001 | 18.7 ± 0.5 | 0.939 |

representing a short non-interfering tag, such as 6x-His tag previously characterized for its impact on CBS protein expression and folding [51]. The affinity of $mNG2_{11}$ fragment to the co-expressed non-fluorescent $mNG2_{1-10}$ fragment (213 residues, ~24 kDa) has not been experimentally determined, but it is believed to be in pM to low nM range [37]. Such high affinity ensures strong complementation of a signal in cells as long as the fragment is exposed and accessible, which is beneficial for folding reporter assays, but is problematic for other applications, such as studying protein–protein interactions, where lower affinity (in high μM range) luciferase-based modified NanoLuc complementation reporter NanoBiT is preferred [52]. Our CBS folding reporter assay showed a clear quantifiable difference between properly folded CBS WT and misfolded CBS I278T variant (Fig. 1). In addition, the assay was successfully validated using proteasome inhibitors as positive controls (Fig. 2). Proteasome inhibitors were studied extensively as potential treatment for HCU using transgenic mouse models expressing various missense pathogenic HCU-causing variants [23,53]. Interestingly, Tg-I278T mice showed heterogeneous response to proteasome inhibitor treatment with some animals responding strongly by increased steady-state levels of CBS protein and its native tetramers in liver homogenates, which translated to substantially decreased plasma tHcy levels, while other animals displayed minimal detectable changes in liver CBS protein levels and plasma tHcy [21]. The reason for this heterogeneous response has not been understood, although differences in effectiveness of proteasome inhibition were ruled out and multiple genes related to steroid hormone metabolism showed substantial difference on transcription level between responding and nonresponding Tg-I278T mice.

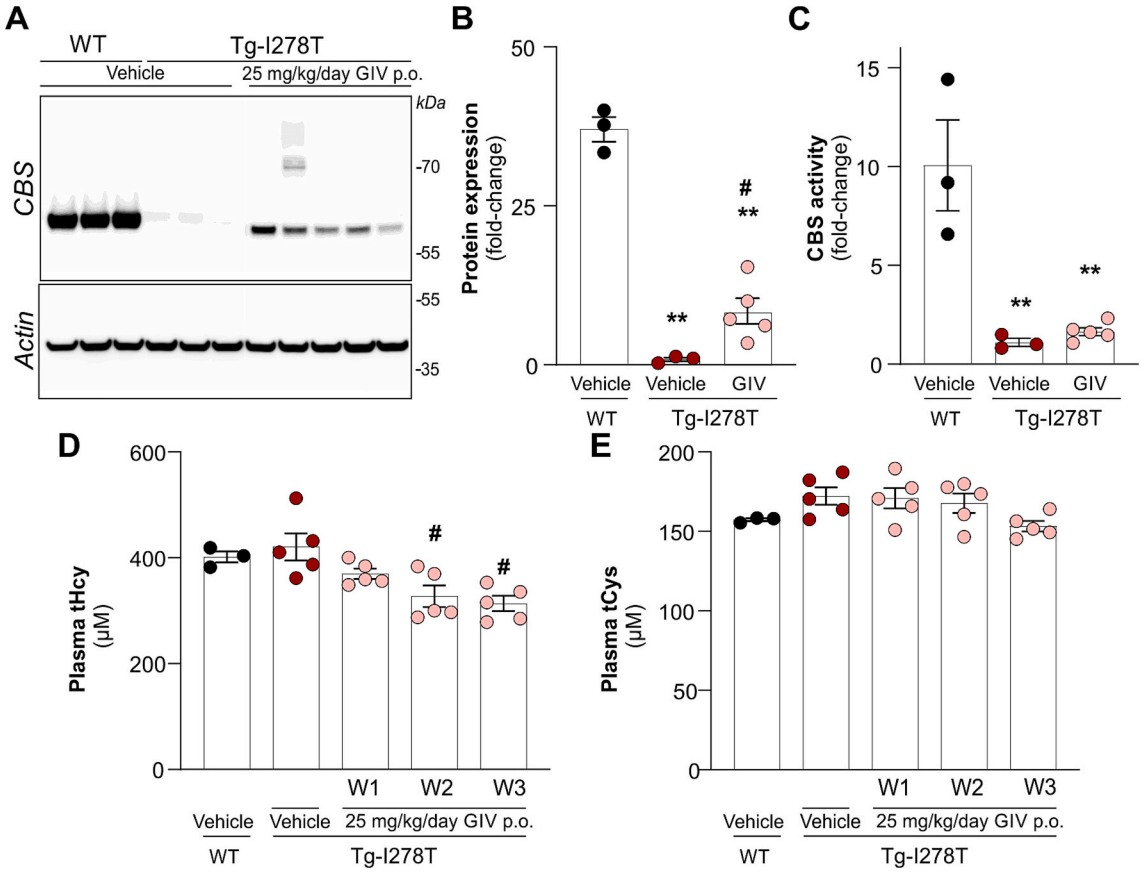


**Fig. 5. Short-term treatment of Tg-I278T HCU mice with givinostat. A&B –** Representative Western blot (**A**) and quantification (**B**) of CBS expression levels in livers collected from the untreated WT controls, vehicle-treated Tg-I278T and Tg-I278T mice treated with givinostat (25 mg/kg/day p.o.) for three weeks. **C –** Relative CBS activities in livers of the samples analyzed in panels **A&B**. **D&E –** Total homocysteine (tHcy, **D**) and total cysteine (tCys, **E**) in serum samples collected throughout the study as described in the Materials and methods section.

In the next step, we used our validated CBS folding reporter assay to screen chemical libraries with compounds that could be potentially considered for therapeutic repurposing or provide suitable scaffolds for further development (Fig. 3). To our knowledge, development of this assay and its use in HTS of chemical libraries represent the first step in systemic search and rational design of pharmacological chaperones for HCU. Previously, we and others have experimented with non-specific chemical chaperones and potential pharmacological chaperones on an individual basis [16–19,54,55]. While these studies supported the notion of HCU being a conformational disorder, they were unfortunately not poised to yield clinically translatable hits. Here, using two libraries with 3,793 compounds in total, we found that ~1% of the tested compounds significantly improved CBS I278T folding; however, only < 0.2% of these compounds showed a combined rescue of protein folding and CBS enzymatic activity in addition to the acceptable pharmacological profile. One group of compounds that stood out from the identified hits were HDAC inhibitors including compounds such as givinostat, resminostat, citarinostat and panobinostat. Given the fact that givinostat resulted in the highest rescue of CBS activity and is an FDA-approved drug for Duchenne muscular dystrophy [47], we selected givinostat for further characterization (Figs. 4 and 5). HDAC inhibitors deactivate histone deacetylases, thus rendering chromatin more transcriptionally active and consequently regulating gene expression. In addition to histones, HDAC inhibitors also affect transcription factor, molecular chaperones and other cytoplasmic proteins, which regulate a variety of transcription-independent processes including proteostasis, folding, degradation and aggresomal formation [47]. For example, vorinostat and the investigational HDAC inhibitor LB-205 prevented rapid degradation and restored the activity of glucocerebrosidase in a model of Gaucher disease, a lysosomal storage disorder [56]. Interestingly, a small chemical chaperone 4-phenylbutyric acid, which was studied for its potential chaperone-like effect on multiple missense pathogenic CBS variants expressed in both *E. coli* and mammalian CHO-K1 cells and demonstrated only marginal impact [55], is also an HDAC inhibitor with an ability to mitigate ER stress [57]. Indeed, givinostat treatment resulted in increased expression levels of molecular chaperones Hsp70 and Hsp40, which facilitate proper folding of proteins and, on the other hand, reduced steady-state levels of small HSPs Hsp27 and Hsp22 (Fig. 4). Initial work studying the impact of chemical chaperones on CBS rescue in yeast model of HCU showed that treatment with ethanol induced expression of Hsp70 and rescued dramatic decrease in steady-state Hsp26 levels, while deletion of Hsp26 resulted in rescue of CBS I278T [7]. These observations resulted in proposal of an equilibrium model where a competition between protein degradation mediated by the Hsp26-ubiquitin–proteasome pathway and Hsp70-mediated protein folding pathway regulates steady-state levels and activity of CBS mutants [53]. Considering the functional similarity between yeast Hsp26 and human Hsp27, decreased levels of Hsp27 after treatment with givinostat could shift the balance towards proper folding and rescue of CBS I278T further facilitated by upregulated Hsp70 (Fig. 4). Fig. 6 summarizes the proposed mechanism of givinostat and likely other HDAC inhibitors compared to proteasome inhibitors. While proteasome inhibitors, such as bortezomib, inhibit degradation of misfolded CBS targeted thus allowing more time for cellular molecular chaperones to fold the CBS polypeptide properly, HDAC inhibitors, such as givinostat, modulate expression levels of HSPs. Downregulation of small HSPs like Hsp27 and Hsp22 leads to a decreased tagging of misfolded CBS polypeptide by Hsp27 and subsequently ubiquitin thus preventing its rapid proteasomal degradation, while upregulation of Hsp70 and its co-chaperone Hsp40 facilitates improved folding and rescue of CBS.

In conclusion, we successfully developed a novel cell-based CBS folding reporter assay and demonstrated its utility in screening for potential pharmacological chaperones for HCU. We identified and evaluated givinostat as a representative of HDAC inhibitors in Tg-I278T mouse model of HCU. Although the pilot 3-weeks-long study showed only ~25% decrease of plasma tHcy levels in the treated Tg-I278T mice, which seems distant from a 100 μM clinically relevant threshold, we believe that these initial results warrant a follow-up in exploring other HDAC inhibitors for better efficacy and longer treatment periods to achieve substantial drop in plasma tHcy levels. Givinostat, a clinically approved drug, is intended for a long-term, potentially lifelong treatment of Duchenne muscular dystrophy. Although the drug is not without

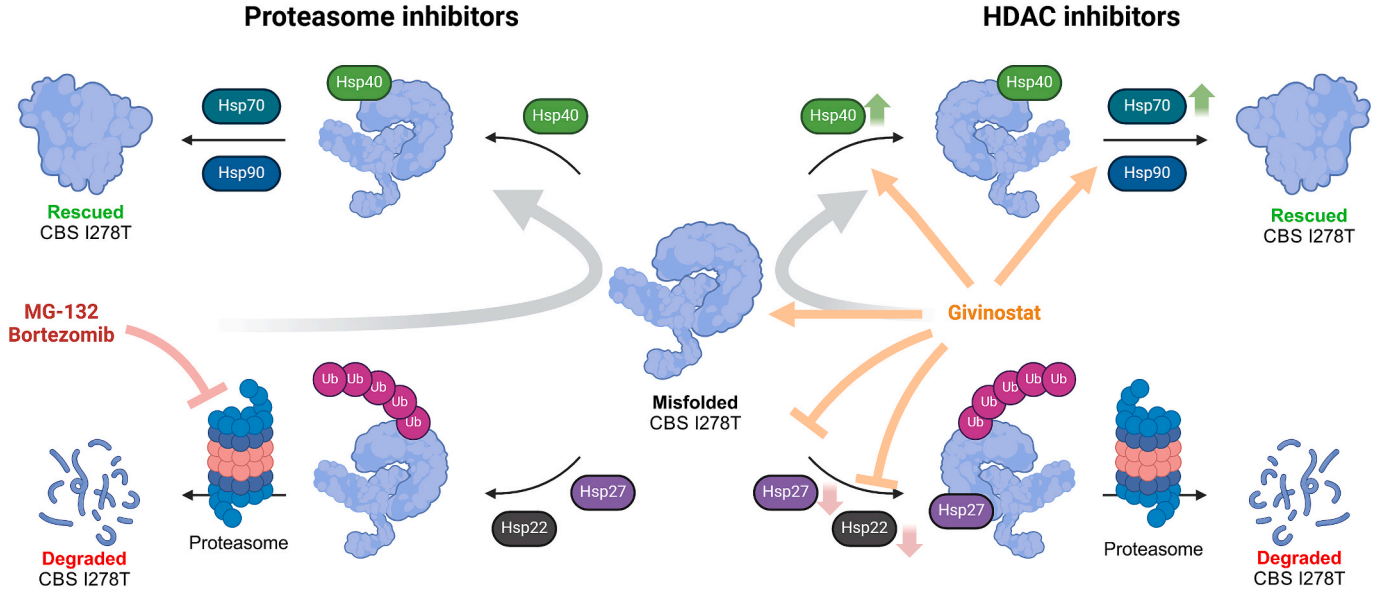


**Fig. 6. Proposed mechanism of action of proteasome inhibitors *versus* HDAC inhibitors as pharmacological chaperones for HCU.** Misfolded CBS I278T may undergo two possible fates: either being rescued by the successful protein folding with the assistance of molecular chaperones (e.g. HSPs) or rapidly degraded by the ubiquitin–proteasome machinery. Proteasome inhibitors, such as MG-132 or bortezomib, block activity of proteasome resulting in an accumulation of ubiquitinated misfolded CBS I278T, which shifts the balance towards protein folding pathway. On the other hand, HDAC inhibitors, such as givinostat, modulate expression and activity of proteostasis network to promote folding rather than protein degradation. This is achieved by downregulation of small HSPs, such as Hsp27 and Hsp22, which facilitate CBS I278T polyubiquitination and subsequent degradation and concurrent upregulation of the main protein folding HSPs, such as Hsp70 and Hsp40, which facilitate proper folding of CBS I278T rescuing its steady-state levels and activity.

side effects – such as gastrointestinal issues (diarrhea, nausea, vomiting, and abdominal pain), fatigue, musculoskeletal pain, thrombocytopenia and metabolic effects, such as increased triglyceride levels [47] – this side effect profile does not appear more severe than many of the currently used HCU therapies. If found safe and effective in long-term studies, particularly for pathogenic CBS variants causing pyridoxine non-responsive severe form of HCU, peroral small molecule drugs, such as givinostat, could represent an additional therapeutic option for management of HCU and a game-changer for many HCU patients worldwide.

## Data availability statement

Data will be made available on reasonable request.

## CRediT authorship contribution statement

**Maria Petrosino:** Writing – review & editing, Methodology, Writing – original draft, Investigation, Visualization, Formal analysis, Validation, Data curation. **Karim Zuhra:** Methodology, Writing – review & editing, Investigation, Writing – original draft, Formal analysis, Visualization, Data curation. **Ela Mijatovic:** Formal analysis, Writing – review & editing, Investigation. **Thilo Magnus Philipp:** Methodology, Investigation, Writing – review & editing, Visualization. **Olivier Bremer:** Writing – review & editing, Investigation. **Kelly Ascenção:** Writing – review & editing, Resources, Methodology. **Csaba Szabo:** Conceptualization, Writing – review & editing, Supervision, Resources. **Tomas Majtan:** Supervision, Conceptualization, Resources, Writing – review & editing, Project administration, Writing – original draft, Funding acquisition.

## Funding

This work was supported by the University of Fribourg Research Pool grant 22–15, HCU Network America global research grant and the Swiss National Science Foundation Project funding 10.001.133 (all to TM).

## Declaration of competing interest

The authors declare the following financial interests/personal relationships which may be considered as potential competing interests: Tomas Majtan reports financial support was provided by HCU Network America. Tomas Majtan reports financial support was provided by Swiss National Science Foundation. Tomas Majtan reports a relationship with Travere Therapeutics Inc that includes: consulting or advisory, funding grants, and travel reimbursement. If there are other authors, they declare that they have no known competing financial interests or personal relationships that could have appeared to influence the work reported in this paper.

## Data availability

Data will be made available on request.

## References

[1] J.P. Kraus, M. Janosik, V. Kozich, R. Mandell, V. Shih, M.P. Sperandeo, G. Sebastio, R. de Franchis, G. Andria, L.A.J. Kluijtmans, H. Blom, G.H.J. Boers, R.B. Gordon, P. Kamoun, M.Y. Tsai, W.D. Kruger, H.G. Koch, T. Ohura, M. Gaustadnes, Cystathionine β-synthase mutations in homocystinuria, Hum. Mutation 13 (1999) 362–375.

[2] K. Zuhra, F. Augsburger, T. Majtan, C. Szabo, Cystathionine-beta-Synthase: Molecular Regulation and Pharmacological Inhibition, Biomolecules 10 (5) (2020) 697.

[3] T. Majtan, T. Olsen, J. Sokolova, J. Krijt, M. Krizkova, T. Ida, T. Ditroi, H. Hansikova, O. Vit, J. Petrak, L. Kuchar, W.D. Kruger, P. Nagy, T. Akaike, V. Kozich, Deciphering pathophysiological mechanisms underlying cystathionine beta-synthase-deficient homocystinuria using targeted metabolomics, liver proteomics, sphingolipidomics and analysis of mitochondrial function, Redox Biol. 73 (2024) 103222.

[4] S.H. Mudd, H.L. Levy, J.P. Kraus, Disorders of transsulfuration, in: C.R. Scriver, A. L. Beaudet, W.S. Sly, D. Valle, B. Childs, K. Kinzler, B. Vogelstein (Eds.), The Metabolic and Molecular Bases of Inherited Disease, McGraw-Hill, New York, 2001, pp. 2007–2056.

[5] V. Kozich, J. Sokolova, A.A.M. Morris, M. Pavlikova, F. Gleich, S. Kolker, J. Krijt, C. Dionisi-Vici, M.R. Baumgartner, H.J. Blom, M. Huemer, E.H. consortium, Cystathionine beta-synthase deficiency in the E-HOD registry-part I: pyridoxine responsiveness as a determinant of biochemical and clinical phenotype at diagnosis, J. Inherit. Metab. Dis. 44 (3) (2021) 677–692.

[6] A.A. Morris, V. Kozich, S. Santra, G. Andria, T.I. Ben-Omran, A.B. Chakrapani, E. Crushell, M.J. Henderson, M. Hochuli, M. Huemer, M.C. Janssen, F. Maillot, P. D. Mayne, J. McNulty, T.M. Morrison, H. Ogier, S. O'Sullivan, M. Pavlikova, I.T. de Almeida, A. Terry, S. Yap, H.J. Blom, K.A. Chapman, Guidelines for the diagnosis and management of cystathionine beta-synthase deficiency, J. Inherit. Metab. Dis. 40 (1) (2017) 49–74.

[7] L.R. Singh, W.D. Kruger, Functional rescue of mutant human cystathionine beta-synthase by manipulation of Hsp26 and Hsp70 levels in Saccharomyces cerevisiae, J. Biol. Chem. 284 (7) (2009) 4238–4245.

[8] L.R. Singh, S. Gupta, N.H. Honig, J.P. Kraus, W.D. Kruger, Activation of mutant enzyme function in vivo by proteasome inhibitors and treatments that induce Hsp70, PLoS Genet. 6 (1) (2010) e1000807.

[9] R. Collard, T. Majtan, Genetic and Pharmacological Modulation of Cellular Proteostasis Leads to Partial Functional Rescue of Homocystinuria-Causing Cystathionine-Beta Synthase Variants, Mol. Cell Biol. 43 (12) (2023) 664–674.

[10] E. Mijatovic, K. Ascencao, C. Szabo, T. Majtan, Cellular turnover and degradation of the most common missense cystathionine beta-synthase variants causing homocystinuria, Protein Sci. 33 (8) (2024) e5123.

[11] W.E. Balch, R.I. Morimoto, A. Dillin, J.W. Kelly, Adapting proteostasis for disease intervention, Science 319 (5865) (2008) 916–919.

[12] F.U. Hartl, M. Hayer-Hartl, Converging concepts of protein folding in vitro and in vivo, Nat. Struct. Mol. Biol. 16 (6) (2009) 574–581.

[13] D. Siva Sankar, J. Dengjel, Protein complexes and neighborhoods driving autophagy, Autophagy (2020) 1–17.

[14] M.L. Tran, Y. Genisson, S. Ballereau, C. Dehoux, Second-Generation Pharmacological Chaperones: Beyond Inhibitors, Molecules 25 (14) (2020).

[15] M.S. Hipp, P. Kasturi, F.U. Hartl, The proteostasis network and its decline in ageing, Nat. Rev. Mol. Cell Biol. 20 (7) (2019) 421–435.

[16] L.R. Singh, X. Chen, V. Kozich, W.D. Kruger, Chemical chaperone rescue of mutant human cystathionine beta-synthase, Mol. Genet. Metab. 91 (4) (2007) 335–342.

[17] T. Majtan, L. Liu, J.F. Carpenter, J.P. Kraus, Rescue of cystathionine beta-synthase (CBS) mutants with chemical chaperones: purification and characterization of eight CBS mutant enzymes, J. Biol. Chem. 285 (21) (2010) 15866–15873.

[18] V. Kozich, J. Sokolova, V. Klatovska, J. Krijt, M. Janosik, K. Jelinek, J.P. Kraus, Cystathionine beta-synthase mutations: effect of mutation topology on folding and activity, Hum. Mutat. 31 (7) (2010) 809–819.

[19] J. Kopecka, J. Krijt, K. Rakova, V. Kozich, Restoring assembly and activity of cystathionine beta-synthase mutants by ligands and chemical chaperones, J. Inherit. Metab. Dis. 34 (1) (2011) 39–48.

[20] J. Adams, Development of the proteasome inhibitor PS-341, Oncologist 7 (1) (2002) 9–16.

[21] S. Gupta, L. Wang, J. Anderl, M.J. Slifker, C. Kirk, W.D. Kruger, Correction of cystathionine beta-synthase deficiency in mice by treatment with proteasome inhibitors, Hum. Mutat. 34 (8) (2013) 1085–1093.

[22] S. Gupta, L. Wang, W.D. Kruger, The c.797 G>A (p.R266K) cystathionine beta-synthase mutation causes homocystinuria by affecting protein stability, Hum Mutat 38(7) (2017) 863-869.

[23] S. Gupta, H.O. Lee, L. Wang, W.D. Kruger, Examination of two different proteasome inhibitors in reactivating mutant human cystathionine beta-synthase in mice, PLoS One 18 (6) (2023) e0286550.

[24] V. Bernier, M. Lagace, D.G. Bichet, M. Bouvier, Pharmacological chaperones: potential treatment for conformational diseases, Trends Endocrinol Metab 15 (5) (2004) 222–228.

[25] T. Majtan, A.L. Pey, J. Ereno-Orbea, L.A. Martinez-Cruz, J.P. Kraus, Targeting Cystathionine Beta-Synthase Misfolding in Homocystinuria by Small Ligands: State of the Art and Future Directions, Curr. Drug Targets 17 (13) (2016) 1455–1470.

[26] P. Leandro, C.M. Gomes, Protein misfolding in conformational disorders: rescue of folding defects and chemical chaperoning, Mini Rev. Med. Chem. 8 (9) (2008) 901–911.

[27] T.G. Lucas, C.M. Gomes, B.J. Henriques, Thermal Shift and Stability Assays of Disease-Related Misfolded Proteins Using Differential Scanning Fluorimetry, Methods Mol. Biol. 2019 (1873) 255–264.

[28] K. Zuhra, P.M.F. Sousa, G. Paulini, A.R. Lemos, Z. Kalme, I. Bisenieks, E. Bisenieks, B. Vigante, G. Duburs, T.M. Bandeiras, L. Saso, A. Giuffre, J.B. Vicente, Screening Pyridine Derivatives against Human Hydrogen Sulfide-synthesizing Enzymes by Orthogonal Methods, Sci. Rep. 9 (1) (2019) 684.

[29] B.W. Ramsey, J. Davies, N.G. McElvaney, E. Tullis, S.C. Bell, P. Drevinek, M. Griese, E.F. McKone, C.E. Wainwright, M.W. Konstan, R. Moss, F. Ratjen, I. Sermet-Gaudelus, S.M. Rowe, Q. Dong, S. Rodriguez, K. Yen, C. Ordonez, J.S. Elborn, V.X. S. Group, A CFTR potentiator in patients with cystic fibrosis and the G551D mutation, N Engl J Med 365(18) (2011) 1663-72.

[30] F. Van Goor, S. Hadida, P.D. Grootenhuis, B. Burton, J.H. Stack, K.S. Straley, C. J. Decker, M. Miller, J. McCartney, E.R. Olson, J.J. Wine, R.A. Frizzell, M. Ashlock, P.A. Negulescu, Correction of the F508del-CFTR protein processing defect in vitro

by the investigational drug VX-809, Proc. Natl. Acad. Sci. USA. 108 (46) (2011) 18843–18848.
[31] L. Foit, G.J. Morgan, M.J. Kern, L.R. Steimer, A.A. von Hacht, J. Titchmarsh, S. L. Warriner, S.E. Radford, J.C. Bardwell, Optimizing protein stability in vivo, Mol. Cell 36 (5) (2009) 861–871.
[32] A.M. Pittman, M.D. Lage, V. Poltoratsky, J.D. Vrana, A. Paiardini, A. Roncador, B. Cellini, R.M. Hughes, C.L. Tucker, Rapid profiling of disease alleles using a tunable reporter of protein misfolding, Genetics 192 (3) (2012) 831–842.
[33] S. Cabantous, T.C. Terwilliger, G.S. Waldo, Protein tagging and detection with engineered self-assembling fragments of green fluorescent protein, Nat. Biotechnol. 23 (1) (2005) 102–107.
[34] W. Chun, G.S. Waldo, G.V. Johnson, Split GFP complementation assay for quantitative measurement of tau aggregation in situ, Methods Mol. Biol. 670 (2011) 109–123.
[35] S. Feng, S. Sekine, V. Pessino, H. Li, M.D. Leonetti, B. Huang, Improved split fluorescent proteins for endogenous protein labeling, Nat. Commun. 8 (1) (2017) 370.
[36] T.J. Nelson, J. Zhao, C.I. Stains, Utilizing split-NanoLuc luciferase fragments as luminescent probes for protein solubility in living cells, Methods Enzymol. 622 (2019) 55–66.
[37] M.G. Romei, S.G. Boxer, Split Green Fluorescent Proteins: Scope, Limitations, and Outlook, Annu. Rev. Biophys. 48 (2019) 19–44.
[38] T. Majtan, A.L. Pey, R. Fernandez, J.A. Fernandez, L.A. Martinez-Cruz, J.P. Kraus, Domain organization, catalysis and regulation of eukaryotic cystathionine beta-synthases, PLoS One 9 (8) (2014) e105290.
[39] M. Petrosino, K. Zuhra, J. Kopec, A. Hutchin, C. Szabo, T. Majtan, H2S biogenesis by cystathionine beta-synthase: mechanism of inhibition by aminooxyacetic acid and unexpected role of serine, Cell. Mol. Life Sci. 79 (8) (2022) 438.
[40] J.P. Kraus, L.E. Rosenberg, Cystathionine beta-synthase from human liver: improved purification scheme and additional characterization of the enzyme in crude and pure form, Arch. Biochem. Biophys. 222 (1) (1983) 44–52.
[41] K. Zuhra, M. Petrosino, B. Gupta, T. Panagaki, M. Cecconi, V. Myrianthopoulos, R. Schneiter, E. Mikros, T. Majtan, C. Szabo, Epigallocatechin gallate is a potent inhibitor of cystathionine beta-synthase: Structure-activity relationship and mechanism of action, Nitric Oxide 128 (2022) 12–24.
[42] L. Wang, X. Chen, B. Tang, X. Hua, A. Klein-Szanto, W.D. Kruger, Expression of mutant human cystathionine beta-synthase rescues neonatal lethality but not homocystinuria in a mouse model, Hum. Mol. Genet. 14 (15) (2005) 2201–2208.
[43] S.A. Licandro, L. Crippa, R. Pomarico, R. Perego, G. Fossati, F. Leoni, C. Steinkuhler, The pan HDAC inhibitor Givinostat improves muscle function and histological parameters in two Duchenne muscular dystrophy murine models expressing different haplotypes of the LTBP4 gene, Skelet. Muscle 11 (1) (2021) 19.
[44] T.M. Philipp, T. Bottiglieri, W. Clapper, K. Liu, S. Rodems, C. Szabo, T. Majtan, Mechanism of action and impact of thiol homeostasis on efficacy of an enzyme replacement therapy for classical homocystinuria, Redox Biol. 77 (2024) 103383.
[45] J.H. Zhang, T.D. Chung, K.R. Oldenburg, A Simple Statistical Parameter for Use in Evaluation and Validation of High Throughput Screening Assays, J. Biomol. Screen. 4 (2) (1999) 67–73.
[46] C. Brideau, B. Gunter, B. Pikounis, A. Liaw, Improved statistical methods for hit selection in high-throughput screening, J. Biomol. Screen. 8 (6) (2003) 634–647.
[47] C. Mozzetta, V. Sartorelli, C. Steinkuhler, P.L. Puri, HDAC inhibitors as pharmacological treatment for Duchenne muscular dystrophy: a discovery journey from bench to patients, Trends Mol. Med. 30 (3) (2024) 278–294.
[48] M. Sellos-Moura, F. Glavin, D. Lapidus, K. Evans, C.R. Lew, D.E. Irwin, Prevalence, characteristics, and costs of diagnosed homocystinuria, elevated homocysteine, and phenylketonuria in the United States: a retrospective claims-based comparison, BMC Health Serv. Res. 20 (1) (2020) 183.
[49] T. Majtan, V. Kozich, W.D. Kruger, Recent therapeutic approaches to cystathionine beta-synthase-deficient homocystinuria, Br. J. Pharmacol. 180 (3) (2023) 264–278.
[50] M.J. Henderson, M.A. Holbert, A. Simeonov, L.A. Kallal, High-Throughput Cellular Thermal Shift Assays in Research and Drug Discovery, SLAS Discov 25 (2) (2020) 137–147.
[51] T. Majtan, J.P. Kraus, Folding and activity of mutant cystathionine beta-synthase depends on the position and nature of the purification tag: Characterization of the R266K CBS mutant, Protein Expr. Purif. 82 (2) (2012) 317–324.
[52] A.S. Dixon, M.K. Schwinn, M.P. Hall, K. Zimmerman, P. Otto, T.H. Lubben, B. L. Butler, B.F. Binkowski, T. Machleidt, T.A. Kirkland, M.G. Wood, C.T. Eggers, L. P. Encell, K.V. Wood, NanoLuc Complementation Reporter Optimized for Accurate Measurement of Protein Interactions in Cells, ACS Chem. Biol. 11 (2) (2016) 400–408.
[53] W.D. Kruger, How to fix a broken protein: restoring function to mutant human cystathionine beta-synthase, Hum. Genet. 141 (7) (2022) 1299–1308.
[54] T. Majtan, L.R. Singh, L. Wang, W.D. Kruger, J.P. Kraus, Active cystathionine beta-synthase can be expressed in heme-free systems in the presence of metal-substituted porphyrins or a chemical chaperone, J. Biol. Chem. 283 (50) (2008) 34588–34595.
[55] P. Melenovska, J. Kopecka, J. Krijt, A. Hnizda, K. Rakova, M. Janosik, B. Wilcken, V. Kozich, Chaperone therapy for homocystinuria: the rescue of CBS mutations by heme arginate, J. Inherit. Metab. Dis. 38 (2) (2015) 287–294.
[56] J. Lu, C. Yang, M. Chen, D.Y. Ye, R.R. Lonser, R.O. Brady, Z. Zhuang, Histone deacetylase inhibitors prevent the degradation and restore the activity of glucocerebrosidase in Gaucher disease, Proc. Natl. Acad. Sci. USA. 108 (52) (2011) 21200–21205.
[57] D.H. Perlmutter, Chemical chaperones: a pharmacological strategy for disorders of protein folding and trafficking, Pediatr. Res. 52 (6) (2002) 832–836.